Inactivation of A Currents and A Channels on Rat Nodose Neurons in Culture

ELLIS COOPER and ALVIN SHRIER

From the Department of Physiology, McGill University, Montreal, Quebec H3G 1Y6, Canada

ABSTRACT Cultured sensory neurons from nodose ganglia were investigated with whole-cell patch-clamp techniques and single-channel recordings to characterize the A current. Membrane depolarization from −40 mV holding potential activated the delayed rectifier current (IK) at potentials positive to −30 mV; this current had a sigmoidal time course and showed little or no inactivation. In most neurons, the A current was completely inactivated at the −40 mV holding potential and required hyperpolarization to remove the inactivation; the A current was isolated by subtracting the IK evoked by depolarizations from −40 mV from the total outward current evoked by depolarizations from −90 mV. The decay of the A current on several neurons had complex kinetics and was fit by the sum of three exponentials whose time constants were 10–40 ms, 100–350 ms, and 1–3 s. At the single-channel level we found that one class of channel underlies the A current.

The conductance of A channels varied with the square root of the external K concentration: it was 22 pS when exposed to 5.4 mM K externally, and increased to 40 pS when exposed to 140 mM K externally. A channels activated rapidly upon depolarization and the latency to first opening decreased with depolarization. The open time distributions followed a single exponential and the mean open time increased with depolarization. A channels inactivate in three different modes: some A channels inactivated with little reopening and gave rise to ensemble averages that decayed in 10–40 ms; other A channels opened and closed three to four times before inactivating and gave rise to ensemble averages that decayed in 100–350 ms; still other A channels opened and closed several hundred times and required seconds to inactivate. Channels gating in all three modes contributed to the macroscopic A current from the whole cell, but their relative contribution differed among neurons. In addition, A channels could go directly from the closed, or resting, state to the inactivated state without opening, and the probability for channels inactivating in this way was greater at less depolarized voltages. In addition, a few A channels appeared to go reversibly from a mode where inactivation occurred rapidly to a slow mode of inactivation.

Address reprint requests to Dr. Ellis J. Cooper, Department of Physiology, McGill University, McIntyre Medical Building, 3655 Drummond Street, Montreal, Quebec H3G 1Y6, Canada.

J. GEN. PHYSIOL. © The Rockefeller University Press · 0022-1295/89/11/0881/30 $2.00
Volume 94 November 1989 881–910

INTRODUCTION

Fast transient K currents, or A currents, activate rapidly upon membrane depolarization, then inactivate and require membrane hyperpolarization to remove this inactivation. A currents were first identified on molluscan neurons (Hagiwara et al., 1961; Connor and Stevens, 1971; Neher, 1971) and are thought to regulate action potential firing frequencies, action potential repolarization, and in some neurons, to modulate excitatory synaptic potentials. Recently, similar currents have been recorded in a variety of cell types, including mammalian neurons. In some preparations it has been difficult to isolate A currents entirely from other voltage-dependent potassium currents in the membrane and, consequently, A currents could be studied only over a limited voltate range. In this paper, we have taken the additional approach of isolating the A current at the single-channel level to characterize its voltage- and time-dependent properties. To date, only a few studies exist on transient, or nonstationary, voltage-activated K currents (Cooper and Shrier, 1985; Marty and Neher, 1985; Kasai et al., 1986; Solc et al., 1987; Hoshi and Aldrich, 1988*a*). Approaches for investigating nonstationary channels have been reviewed by Aldrich and Yellen (1983).

Studies of A currents indicate that the volatge range for activation and inactivation are fairly consistent among neurons (i.e., Connor and Stevens, 1971; Neher, 1971; Gustafsson et al., 1982; Segal and Barker, 1984; Belluzi et al., 1985; Zbicz and Weight, 1985), however, there are large variations in the reported kinetics of A current inactivation, even for neurons of the same type and from the same species. For example, Kostyuk et al. (1981) reported that A currents on rat dorsal root ganglion (DRG) neurons inactivate with a single exponential time course whose time constant was voltage dependent and measured 150 ms at -20 mV and decreased to ~90 ms at potentials >0 mV. In contrast Mayer and Sugiyama (1988), who also studied rat DRG neurons, reported kinetics for A currents that are more complicated and have at least three components: a fast component whose time constant is in the range of 5–8 ms, a slow component whose time constant is in the range of 40–50 ms, and a much slower component that was not measured but appears from their records to be in the order of seconds. The reasons for the complex kinetics of the A current is unclear, but simialr variablitity has been reported for other types of neurons, for example, guinea pig hippocampal pyramidal neurons (compare Gustafsson et al., 1982; Zbicz and Weight, 1985; and Numann et al., 1987).

To learn more about the inactivation of A currents, we have studied the A current on cultured sensory neurons isolated from nodose ganglia of rats. In this paper, we show that the complex inactivation of the A current is a result of the individual channels inactivating in different modes.

METHODS

Cell Culture

Nodose neurons were dissected from newborn rats (C.D. strain, Charles River, Canada) killed by cervical dislocation. The ganglia were dissociated with enzyme-containing media (Dispase, grade 1, 1 mg/ml; Boehringer Mannheim Inc., Indianapolis, IN), and the neurons were cultured at 37°C in a 5% CO_2 environment according to methods described previously (Cooper,

1984). The culture media consisted of L-15 (Flow Laboratories, Inc., Rockville, MD) supplemented with vitamins and cofactors, rat serum (5%), and 7S nerve growth factor purified by us from male mouse submaxillary glands (Bocchini and Angeletti, 1969) and the neurons were grown on Aclar (Allied Chemical Corp., Waltham, MA) coverslips coated with rat tail collagen.

Recordings

Whole-cell and single-channel patch-clamp techniques (Hamill et al., 1981) were used to record currents from over 150 neurons that had developed for 10–35 d in culture. All experiments were done at room temperature (21–24°C) with either a List EPC-7 or a home built voltage-clamp circuit, as described by Hamill et al. (1981), that had a fixed 500-MΩ feedback resistor for whole-cell recording and a 10-GΩ feedback resistor for single-channel recording. The pipette resistances were 2–6 MΩ and the current signal was balanced to zero with the pipette immersed in the bathing solution. The seal resistances were 5–100 GΩ. The series resistances were usually compensated by the method of Sigworth (1983) when recording whole-cell currents and had values of ~6–10 MΩ.

Whole-Cell Currents

For whole-cell recording, the currents were stable and permitted subtraction techniques for obtaining the A current. To isolate the A current, steps from −40 mV holding potential were subtracted from steps to the same depolarized potentials from −90 mV holding potential, and then a step from −40 to −90 mV was added to the result. (The depolarizing series from −40 and −90 mV were done within 3 min of each other and we never saw "run down" or other changes in the evoked currents over this time period). The leakage and capacitance currents were usually linear and for IK these currents were corrected for digitally by subtracting the current response to a hyperpolarizing voltage step from an equivalent amplitude depolarizing step. Some nodose neurons have tetrodotoxin-resistant sodium currents (Baccaglini and Cooper, 1982; Bossu and Feltz, 1984; Ikeda and Schofield, 1987), however, only neurons with greatly reduced or completely blocked inward currents were included in this study. Furthermore, as this study deals only with nonregenerative outward currents of relatively small amplitudes (<3 nA), the contribution of outward current from distal unclamped regions is low and does not significantly affect our results; any neuron in which there was a suggestion of poor clamping, such as notches, oscillations, or delayed all-or-none inward currents, was excluded.

Single-Channel Currents

For single-channel measurements, all recordings were made in cell-attached configurations. Patch potentials are expressed as membrane potentials by subtracting the pipette potential from −60 mV. (The mean value of the resting potential for nodose neurons in culture was −59.7 ± 5.3 SD [n = 29] determined with patch electrodes.) All records, except where indicated, were corrected for capacity transients and leakage currents by subtracting an average of steps to the same potential in which no channel openings occurred; usually at least 16 records were needed to make a good template for subtraction.

Data Recording and Analysis

During experiments, membrane current and voltage were filtered at 10 kHz and digitized at 44 kHz by a pulse code modulation unit (PCM; Sony Corp., Japan) and recorded on a Beta casette recorder (Sony SL 9100 or H900). During off-line analysis membrane currents were filtered at 0.1–2 kHz through an 8-pole Bessel filter, digitized at 0.2–10 kHz by a 12-bit A/D

converter controlled by a PDP 11/23 or 11/73 (Digital Equipment Corp., Marlboro, MA) and written into data files. Measurements and curve fitting were carried out on the DEC computers. A least-squares method was used for exponential fitting to the data (Hunter and Kearney, 1984) and both experimental and theoretical curves were simultaneously displayed. The overall goodness of fit was given by the variance accounted for, and the AIC criteria (Akaike, 1974) was used to determine which exponential fit was the most appropriate model of the data. Tail current records were fit after the decay of the capacity current and extrapolated back to the time the voltate step was made.

In this paper, a computer routine that fits single channels with idealized square pulses was used for single-channel measurements of current amplitudes, open times, and closed times. This routine was not accurate when two or more channels were open simultaneously, and in these cases the idealized square pulse was adjusted by eye with cursors. When the opening of two channels overlapped, we assumed that the channel that opened first closed first 50% of the time (Aldrich et al., 1983); in the rare occurrence that three or more openings overlapped no attempt was made to measure open times. All values were stored on file for later use. Depolarizing steps were usually made sufficiently long so that it was rare for events to be open at the end of the step; <5% of the events were in this category. Because the number of these events was small and because each of these events had different latencies measured from the beginning of the step, which suggests that their contribution to the open-time histogram would be approximately evenly distributed (i.e., not weighted to a particular bin), no correction was made to account for them.

Nonparametric statistics of the Kolmogorov-Smirnov type were used to compare histograms (Conover, 1980).

Solutions

The normal extracellular media contained 140 mM NaCl, 5.4 mM KCl, 1.8 mM $CaCl_2$, 0.18 mM $MgCl_2$, 10 mM HEPES (British Drug House) (pH adjusted with NaOH), 5.6 mM glucose, and 0.07 mM choline chloride. The pH was 7.3–7.4. Tetrodotoxin (Calbiochem Behring Corp., La Jolla, CA) (1 μM) was added to the media to block the Na current. Cobalt (1–3 mM) or cadmium (0.5–1.0 mM) was added to block Ca currents: in some experiments $CaCl_2$ levels were also reduced 0.4 mM. For whole-cell recording, the patch electrode contained 10 mM NaCl, 140 mM KCl, 10 mM HEPES (pH adjusted with KOH), 5 mM glucose, 0.5 mM $MgCl_2$, 1–2 mM EGTA, and 0.2 mM $CaCl_2$ to give a final [Ca] of $\sim 10^{-7}$ M; pH was 7.3–7.4. For single-channel measurements, the media in the recording pipette was the same as the extracellular media in most experiments, but in other experiments it contained either 30, 60, or 140 mM KCl, which was achieved by decreasing NaCl by the equivalent amount. In still other experiments, [Ca] was lowered to $\sim 10^{-7}$ M.

RESULTS

Whole-Cell Currents

When cultured nodose neurons are exposed to pharmacological agents that block inward Na and Ca currents, membrane depolarizations from −40 mV holding potential (Vh) evoke only outward currents. A typical example is shown in Fig. 1 *A*. This current activates at potentials more positive than −20 mV with a sigmoidal time course and shows little inactivation, at least up to +50 mV. Upon returning to the holding potential, the current deactivates and relaxes exponentially to zero (the tail current). Currents like those shown in Fig. 1 *A* were seen in all nodose neurons examined and because they have several characteristics that are similar to delayed

rectifier currents, or IK, in other cells, we refer to this current as the delayed rectifier.

In neurons where the only time-dependent outward current found was IK, holding at voltages more hyperpolarized than −40 mV did not modify the amplitude or time course of the IK evoked during depolarizing voltages (see Fig. 3 *D*); this indicates that steady holding at −40 mV does not cause any inactivation of IK. Furthermore, this delayed rectifier does not even inactivate during long 8–10-s voltage steps (see Fig. 4).

In 24 out of 38 neurons, depolarizing voltage steps activated an additional out-

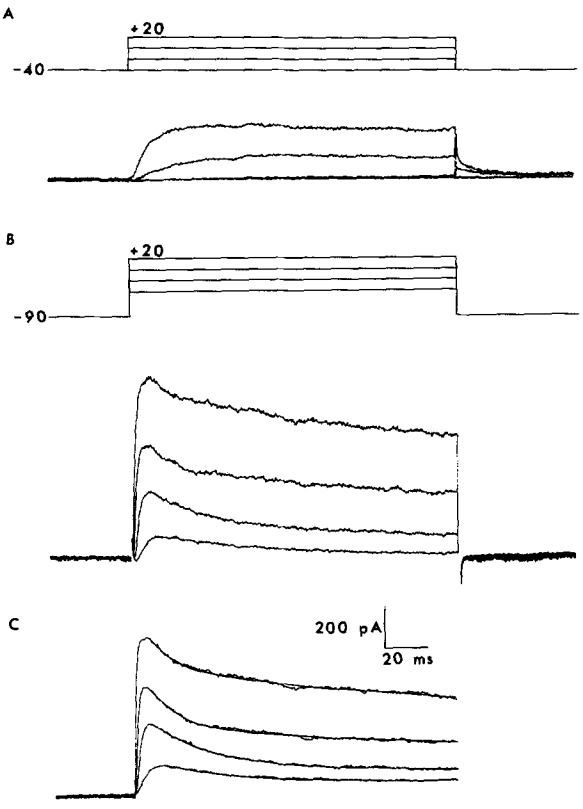

FIGURE 1. Isolation of the A current. *A* shows the IK activated by depolarizing steps from −40 mV to potentials between −20 and +20 mV. *B* shows the total time-dependent outward current activated by depolarizing steps from −90 mV to the same potentials as in *A*. *C* shows the A current in isolation obtained by subtracting the IK current from the total outward current for each step made to the same potential as described in the Methods. The solid lines superimposed on the data represent curves drawn as the sum of two exponentials whose time constants are: −40 mV, 38 ms (0.82) and 323 ms (0.18); −20 mV, 24 ms (0.75) and 339 ms (0.25); 0 mV, 19 ms (0.51) and 348 ms (0.49); 20 mV, 18 ms (0.21) and 330 ms (0.79). In this figure and in subsequent figures time constants are given with the normalized initial amplitude in brackets.

ward current when the membrane was held at hyperpolarized potentials. To determine this additional current in isolation of IK, IK was subtracted from the total current evoked at −90 mV for steps made to the same potential; this difference, which we define as the A current, represents the current that is inactivated at −40 mV holding potential but not at −90 mV. A currents have kinetics that are distinct from IK in that they activate more rapidly than IK and then inactivate. An example is shown in Fig. 1.

As shown in Fig. 1, the peak A current increases with membrane depolarization.

The magnitude of the A current, however, varied widely from neuron to neuron, even within the same culture; the range varied between 315 pA to 1,285 pA at +50 mV, with a mean of 738 ± 142 (mean ± SD). Fig. 2 shows the relationship between peak A current and membrane potential for six neurons. For each neuron, the currents at different potentials are expressed as a percentage of the peak current at +50 mV to facilitate the comparison among neurons. The A current activates at −50 mV and appears to saturate at large depolarizations (+40 to +50 mV). The conductance change corresponding to the peak current was determined by dividing the peak current by the driving force ($V_m - E_k$); the resulting conductance-membrane potential relationship was sigmoidal with a maximum between +20 and +30

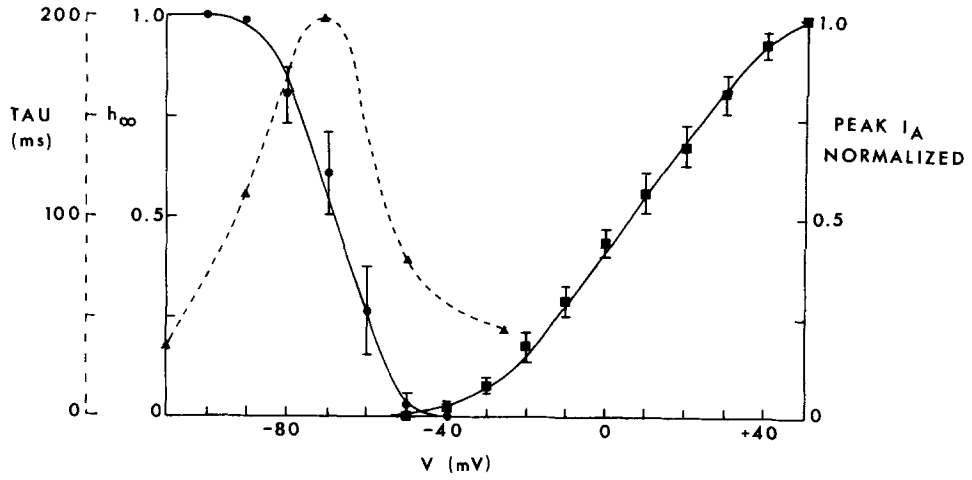

FIGURE 2. Voltage dependence and kinetics of the A current. The squares represent the peak A current evoked by steps from −90 mV to a series of potentials between −50 and +50 mV and are expressed as a fraction of the peak A current at +50 mV for each neuron. The data are the mean of six neurons ± SEM and the points were fit by a line drawn by eye. The line through the circles represents the steady-state inactivation curve, h_∞, and was determined by measuring the peak current evoked by depolarizing steps from different holding potentials; the peak A current evoked from each holding potential is expressed as a fraction of the maximum peak A current. The data are the mean of six neurons ± SD, and the solid line was drawn according to Eq. 1 (see text). The triangles show the time constants for the development and removal of inactivation, which were determined according to protocols described in the text. The bell-shaped curve (*dashed line*) was a fit drawn by eye.

mV and was well fit by the Boltzman distribution (Eq. 1) with $V' = -10$ mV and $k = 8$, which suggests that three gating particles are involved in activation.

$$G/G_{max} = \frac{1}{1 + \exp\left(\frac{V' - V_m}{k}\right)} \quad (1)$$

where $k = KT/ze$, z is the valency of the gating charge, e is the elementary charge, K is the Boltzman constant, T is the absolute temperature, and V' is the voltage at half-maximal conductance.

The relationship between the extent of inactivation and membrane potential was determined by making depolarizing voltage steps to +20 mV from different holding potentials and expressing the peak A current evoked at each holding potential (after subtracting the IK current evoked when holding at −40 mV and stepping to +20 mV) as a fraction of the maximum peak A current. An example from six neurons is shown in Fig. 2. This curve shows that inactivation is fully removed at −90 mV; the relationship is well fit by the Boltzman distribution (see Eq. 1), with $V' = -68$ mV and $k = -8$ as shown by the solid line in Fig. 2.

In five other neurons, in which complete steady-state inactivation curves were not made, we observed that a small fraction (~5%) of the A current still persisted at −40 mV but was totally inactivated at −20 mV; we presume that this shift in steady-state inactivation was due to the high level of divalent cations that we used to block inward currents (Mayer and Sugiyama, 1988).

Both the development and the removal of inactivation take time. The kinetics for these processes were measured with a two-step protocol: for the time course of the development of inactivation, the membrane potential was held at −90 mV and first stepped to an intermediate potential (either −50 or −25 mV) for different durations and then stepped up to 0 mV; the peak current at 0 mV is expressed as a function of the time at the intermediate potential. The time course for removal of inactivation was determined by a similar protocol: the membrane was held at −40 mV and first hyperpolarized to either −70, −90, or −110 mV for different durations and then stepped up to 0 mV; the peak current at 0 mV is expressed as a function of the duration of the hyperpolarization. The time constant for the development and removal of inactivation as a function of the membrane potential of the first step is superimposed on the peak activation and steady state inactivation curves shown in Fig. 2; the function is bell shaped with a peak at approximately −70 mV.

Decay of the A Current

The decay of the A current shown in Fig. 1 had complex kinetics. This observation was true for the majority of neurons (16 of 24) and the A current inactivation was usually fit by the sum of two or, in some neurons, three exponentials whose time constants differed by an order of magnitude (see Fig. 3 *B* and Fig. 4 *A*); the relative contribution of each component, however, varied widely from neuron to neuron as shown in Fig. 3. In the extreme, we observed neurons (2 of 24) whose A current decayed with a single exponential time course (τ = 10–40 ms), as shown in Fig. 3 *A*. And, in other neurons (4 of 24) the A current lacked a rapidly decaying component and was fit by the sum of two exponentials (τ = 150–350 ms and τ = 1–3 s) as shown in Fig. 3 *C*. Fig. 3 *D* shows an example of a cell without an A current.

The experiment illustrated in Fig. 4 shows that slower components of the A current deactivate rapidly when returning the membrane potential to −40 mV, but it can still make a significant contribution to the total outward current for several seconds upon subsequent depolarization. In this way the slow component of the A current may be mistaken as a delayed rectifier current. For example, Fig. 4 *A* shows membrane currents evoked by depolarizing steps from −40 mV holding potential and −90 mV holding potential and illustrates that delayed rectifier has little inacti-

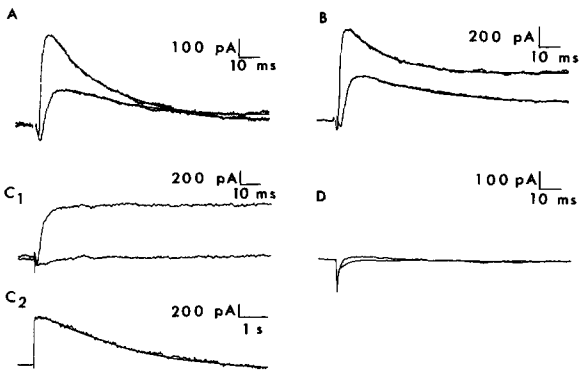

FIGURE 3. Representative A currents. This figure shows A currents from four different neurons *A*, *B*, *C*, and *D*. A pair of A currents are shown for each neuron, one evoked by a step to −20 mV (*lower*) and the other by a step to +20 mV (*upper*). The A currents in this figure were isolated by subtracting the current evoked by steps from −40 mV from the total current evoked by steps to the same potential from −90 mV (see Methods). C_2 shows an additional record of the step to +20 mV on a much slower time scale for the neurons shown in C_1. The solid lines superimposed on the data represent exponential fits of the data whose time constants are *A*: −20 mV, 46 ms; +20 mV, 28 ms; *B*: −20 mV, 57 ms (0.60) and 1,039 ms (0.40); +20 mV, 22 ms (0.59) and 1,071 ms (0.41). C_2: +20 mV, 3,020 ms.

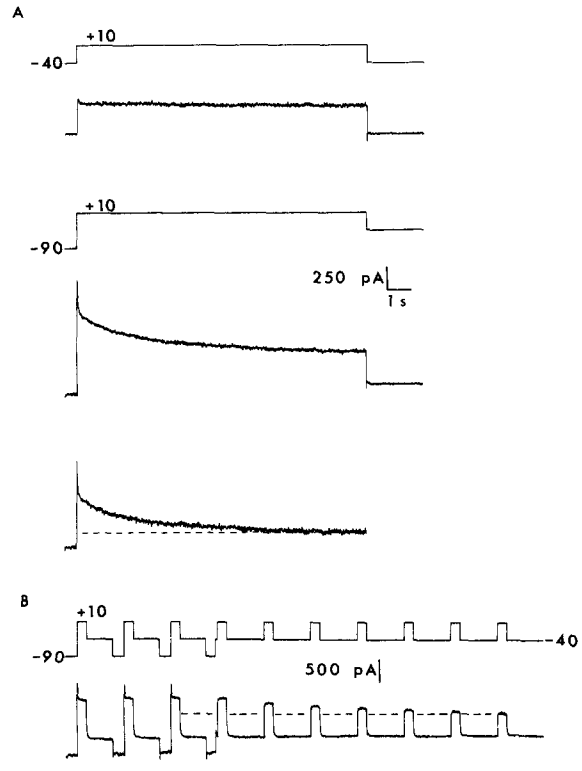

FIGURE 4. Persistent A current due to slow inactivation. *A* shows IK evoked by a 10-s step from −40 to +10 mV (*top*), the total current evoked by a step from −90 to +10 mV (*middle*), and the A current obtained by subtracting the IK from the total current (*bottom*). The solid line superimposed on the data represents a curve drawn as the sum of three exponentials whose time constants are 22 ms (0.40), 273 ms (0.15), and 3,010 ms (0.45). *B* shows the total current when the membrane is hyperpolarized from −40 to −90 mV for 500 ms and then stepped to +10 mV for 400 ms. This protocol was repeated three times and on the fourth step the membrane was stepped from −90 mV back to −40 mV for 130 ms before stepping to +10 mV. The rapid and slow components were present on the first three steps, but the rapid component is absent from the fourth step. Subsequent steps from −40 to +10 mV revealed the slow component which progressively declines as it inactivates. The dashed line represents the level of outward current remaining (IK) after the slow component of the A current inactivates.

vation over 10 s, whereas the A current inactivates. Fig. 4 *B* shows that prepulses to −40 mV can inactivate the rapid component and subsequent depolarizing steps from −40 mV reveals the inactivation of the slow component.

This figure also illustrates that the technique used to isolate A currents can sometimes erroneously subtract the slow components leaving only the rapidly inactivating components. For example, if the fourth step in Fig. 4 *B* is mistakenly considered as only giving rise to delayed rectifier currents and is subtracted from the third step in Fig. 4 *B* to isolate the A current, then only the rapidly decaying component would be revealed and the slow component, which is evident in Fig. 4, *A* and *B*, would be missed. A lack of clear separation between delayed rectifier currents and A currents may, in part, lead to some of the variability that exists in the literature for the kinetics of A current inactivation.

Single A Channels

From the macroscopic currents, it is evident that the time course of the A current inactivation is complex and contains fast components that decay in a few tens of milliseconds, a moderate component that decays in a few hundreds of milliseconds, and a slow component that decays in the order of seconds. The variability in the inactivation time course of the A current between neurons appears to reflect the different contributions of each component to the total outward current.

To further understand the inactivation of the A current, we have isolated, in cell-attached patches, the single channels that underlie the A current in these neurons. A channels were identified by four criteria: (*a*) the current through the channels were carried by potassium, (*b*) the channels activated rapidly upon membrane depolarization to +20 or +30 mV, their appearance was transient and the channels inactivated, (*c*) the channels were inactivated by steady holding at membrane potentials more positive than −40 mV and required membrane hyperpolarization to remove the inactivation, and (*d*) ensemble averages of records containing A channels were similar to macroscopic currents.

Approximately 60% (71 of 113) of cell-attached patches from the neurons' cell body had A channels, and most patches contained three or more A channels. Some patches contained other single-channel currents that differed from A channels in their conductance and in that they did not inactivate. These channels were not studied further and patches containing these channels were not included in the analysis.

Fig. 5 *A* shows examples of single A channels recorded from a cell-attached patch. A channels open rapidly when the membrane is depolarized to +20 mV. When activated, the channels usually open once or twice before undergoing inactivation and require membrane hyperpolarization to remove the inactivation. The reversal potential for the channels was measured in four different extracellular K concentrations (5.4, 30, 60, and 140 mM), and as shown in Fig. 5 *B*, it shifted ~60 mV for a 10-fold change in K concentration in the electrode. This is consistent with K being the main charge carrier for this channel (Taylor, 1987). With 5.4 mM K in the electrode, the single-channel currents did not reverse, and therefore the reversal potential (−85 mV) was estimated by extrapolation.

The single-channel conductance when recorded with 5.4 mM K in the electrode

was 22 pS, but increased to 40 pS when the electrode contained 140 mM as shown in Fig. 5 *C*. The relationship between single-channel conductance and K concentration was not linear, but appeared to follow a square root relationship. In addition, in some records, such as those indicated by the arrows in Figs. 7 and 11, the channel

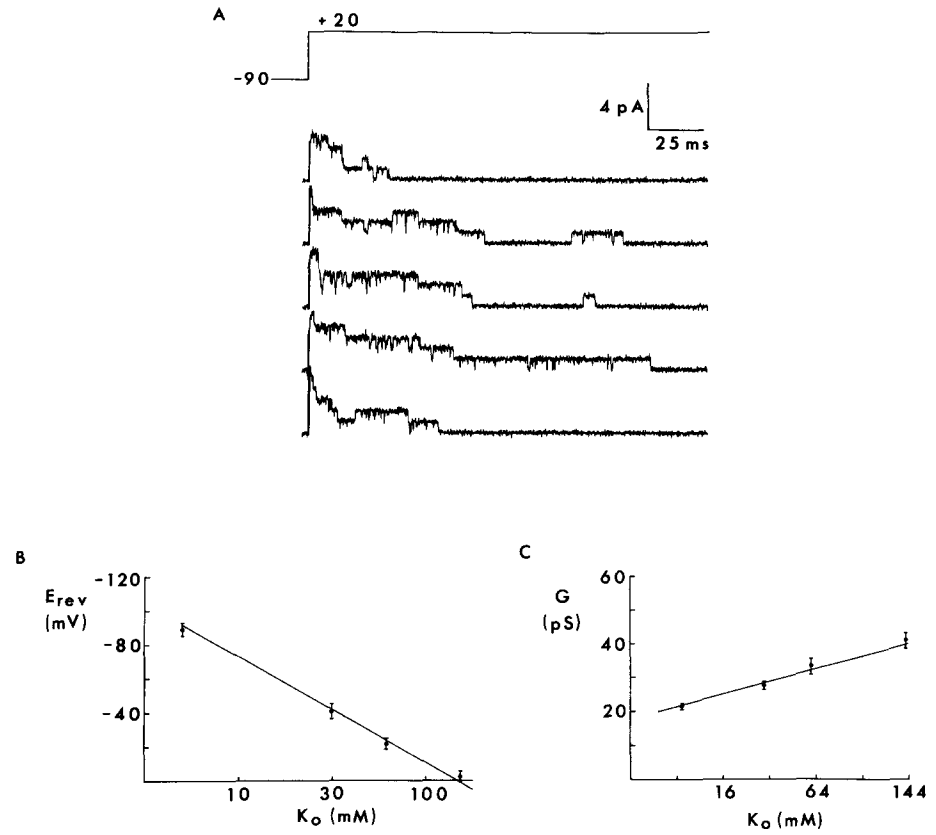

FIGURE 5. Single A channels. *A* shows five consecutive records of single A channels evoked by voltage steps from −90 to +20 mV. The recording electrode contained 140 mM K and the records were filtered at 1.25 kHz and sample at 2.5 kHz. *B* shows the reversal potential (extrapolated for 5.4 mM K) for four different K concentrations. Each point is the mean of at least five different patches and the error bars represent the SEM (for 5.4 mM K $n = 9$ and 140 mM K $n = 8$). The points were joined by a line with a slope of 60 mV/decade. *C* shows the effects of external K on the single-channel conductance. The conductance is plotted against the square root of the external K concentration and each point shows the mean and SEM (the n values are the same as in *B*). A straight line drawn by eye joins the points.

opened or closed to a subconductance state; however, the frequency of observing the substate in any given patch was low.

Fig. 6 shows the ensemble average of channels in another patch activated by a series of 50–60 consecutive steps, each series to a different voltage level, −30, −10, +10, and +30 mV. As can be seen in Fig. 6, these ensemble averages have clear

properties of voltage-dependent activation and inactivation. As the step is made more depolarized the rising phase of the ensemble average becomes faster, the peak current becomes more apparent, the time to peak occurs sooner, the initial decay of the current becomes faster, and there is an apparent steady current at the end of the step, which reflects that A channels inactivate in slower modes (as will be described in more detail below). The decays of these ensemble averages were fit by the sum of three exponentials (see Fig. 6). All these properties are similar to macroscopic A currents.

Open Channel Probability

Most patches in this study contained three or more channels and, as such, complicated measurements of closed times and the probability of reopening for an individual channel (reviewed by Aldrich and Yellen, 1983). In a few experiments, however, a patch contained only one channel. These patches were analyzed further to learn more about properties that affect the inactivation of these channels. Records from the most complete patch are shown in Fig. 7. In this experiment, the patch was depolarized to two levels to learn about the voltage dependence of the latency to first opening, the open times, the closed times, and the number of reopenings per step. Fig. 7 shows a series of consecutive traces in response to voltage steps to +30 mV (left) and to −30 mV (right). The ensemble averages are also shown below each

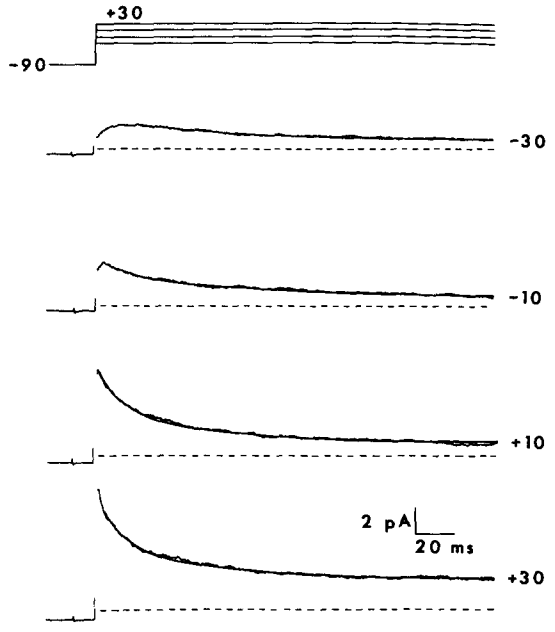

FIGURE 6. Activation. The membrane patch, recorded in cell-attached mode and containing six to seven A channels, was repeatedly stepped to four different potentials, −30 mV, −10 mV, +10 mV, and +30 mV, all from a holding potential of −90 mV. For each potential, 50 to 60 steps were delivered at a rate of 0.5/s. The records in this figure represent the ensemble average for each potential; the dotted line indicates zero current. The solid line superimposed on the data represents exponential fits of the data whose time constants are: −30 mV, 33 ms (0.58) and 310 ms (0.42); −10 mV, 33 ms (0.55), 130 ms (0.15) and 250 ms (0.30); +10 mV, 16 ms (0.51), 105 ms (0.30), and 985 ms (0.19); +30 mV, 12 ms (0.47), 106 ms (0.27), and 2,409 ms (0.26). The recording electrode contained the same media as the extracellular solution. For each average the records were filtered at 1.5 kHz and sampled at 3 kHz.

series in Fig. 7. Of the 282 voltage steps to +30 mV only 8% failed to evoke channel openings, and of the remaining 92%, not one step had two or more channels open simultaneously. These data strongly suggest that this patch contained only one channel. However, as many steps had more than one opening separated in time, the data were further tested for the number of channels in the patch with the binomial distribution (on the assumption that A channels make up a homogeneous population

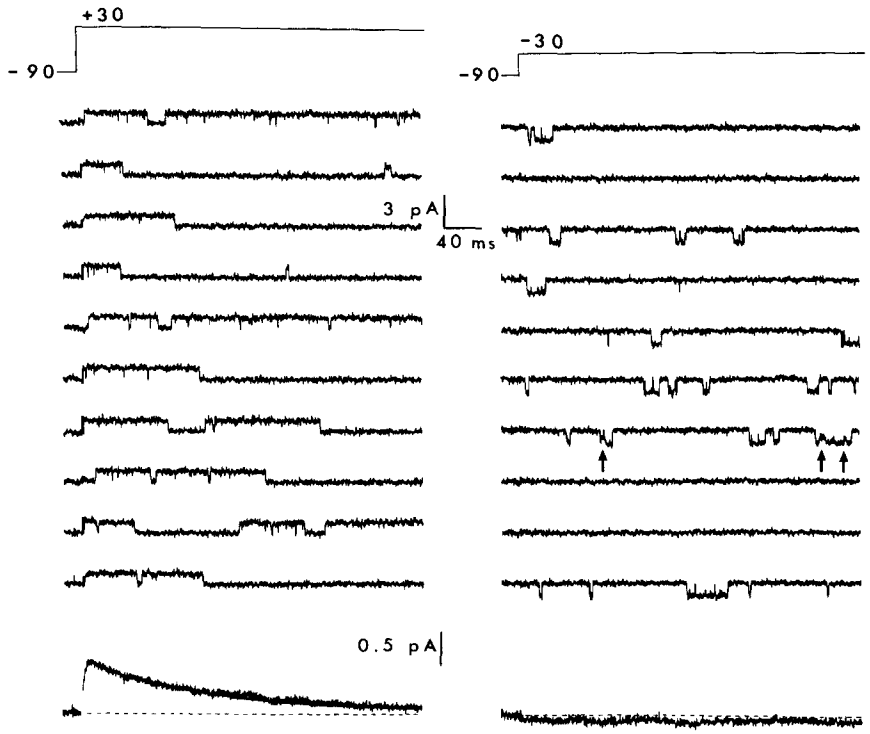

FIGURE 7. Patch containing a single A channel. This figure shows 10 consecutive current traces in response to voltage steps to +30 mV (*left*) and to −30 mV (*right*). The holding potential was −90 mV and the recording electrode contained 140 mM K i.e., E_K = 0 mV, and, as a result, the single-channel currents open upwards (outwards) at +30 mV and downwards (inwards) at −30 mV. The arrow indicates substates. Below each series is the ensemble average of 282 steps to +30 mV and 198 steps to −30 mV. The dotted line represents the zero current level. The solid line through the ensemble average of steps to +30 mV was drawn from a single exponential with a time constant of 153 ms. The records were filtered at 1.5 kHz and sampled at 5 kHz.

and that two or more A channels would gate independently) (Patlak and Horn, 1982; Standen et al., 1985):

$$p_x(t) = \frac{N!}{x!\,(N-x)!}\,p(t)^x q(t)^{(n-x)} \tag{2}$$

where $p_x(t)$ is the probability that x channels are open simultaneously as a function

of time, N is the number of channels in the patch, $p(t)$ is the probability that any given channel will be open as a function of time, and $q(t) = 1 - p(t)$.

The time course of $p(t)$ is given by the ensemble average, but one needs to know N to determine its magnitude. By assuming different values of N and solving Eq. 2 for $p_x(t)$, the only model that was consistent with our data was a patch that contained one channel. Values of $N > 1$ predict that given the number of repeated steps to +30 mV we should have detected two or more channels open simultaneously on a number of steps, especially near the beginning of each step where the probability for opening is highest.

The peak of the ensemble average gives the maximum probability that the channel will be open, which for the patch shown in Fig. 7 is 0.7 and occurs <5 ms after the step to +30 mV (a potential close to the maximum for A current activation). In other patches the maximum probability varied from 0.6 to 0.7.

First Latency

Cumulative histograms of first latency for the patch shown in Fig. 7 are shown in Fig. 8 and demonstrate that the channel opens faster upon greater depolarizations.

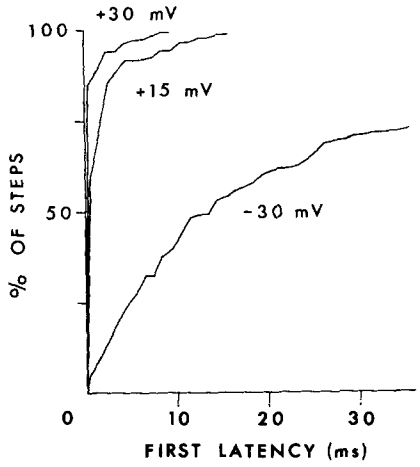

FIGURE 8. First latencies. This figure shows the cumulative histograms of first latencies for the channel shown in Fig. 7 when the patch was depolarized to +30 mV, +15 mV, and −30 mV. The first latency was measured from the beginning of the voltage step to the opening of the channel. The number of latencies measured at each potential was 282 for +30 mV, 73 for +15 mV, and 198 for −30 mV.

In 82% of the steps to +30 mV the channel opened within 2 ms and in 97% the first latencies occurred within 5 ms (not counting the 8% in which channels did not open). For steps to −30 mV, however, activation was much slower; the latency at 50% of the plateau value was 11.5 ms. Also shown in Fig. 8 are the latencies for steps to +15 mV which were not quite as brief as latencies for the +30-mV step. These values of first latencies are similar to Kw channels on PC12 cells (Hoshi and Aldrich, 1988*b*), which also open rapidly and whose first latencies are steeply voltage dependent.

The asymptote of the first latency distribution at −30 mV reached a plateau at 75%, suggesting that the channel may go directly from the closed, or resting, state to the inactivated state without opening (Aldrich et al., 1983); this point was confirmed with a two-step protocol on other patches (see below).

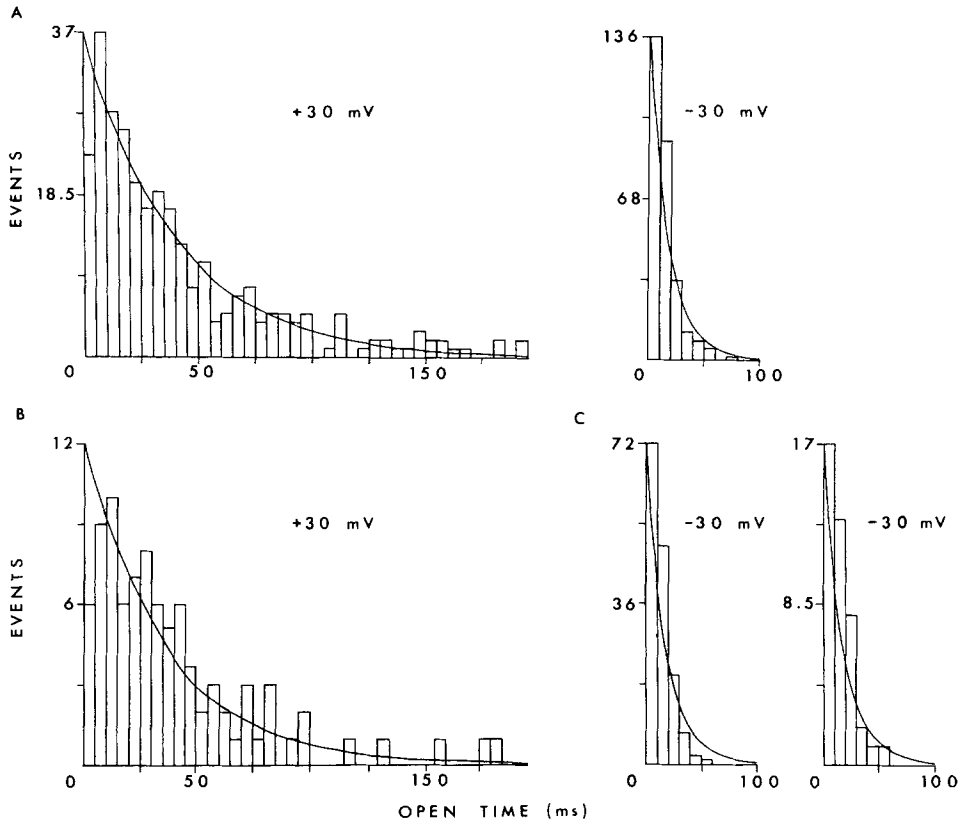

FIGURE 9. Open times. *A* shows histograms of open times for the channel shown in Fig. 7 at two different potentials, +30 mV (*left*) and −30 mV (*right*). The solid line represents single exponential curves with time constants equal to 42 ms for +30 mV and 19 ms for −30 mV. Neither histogram differs significantly (Lilliefors test, 5% level) from the superimposed single exponential. *B* shows the histogram of open times for only those events at +30 mV in *A* that opened at times >30 ms after the depolarizing step. There were 93 such openings and most of these represent reopenings of the channel. This histogram is not significantly different (Lilliefors test, 5% level) from a single exponential with a time constant of 38 ms (*solid curve* in *B*), and is also not significantly different (Smirnov test, 5% level) from the histogram of the total population shown in *A*. *C* shows histograms of open times at −30 mV after the patch had first been depolarized to +30 mV for 50 ms. The histogram on the left in *C* shows open times for the total population ($n = 161$), and the histogram on the right in *C* shows open times for only those events that were open at the time the membrane was stepped back from +30 to −30 mV ($n = 53$). Neither histogram is significantly different (Lilliefors test, 5% level) from a single exponential with a time constant of 19 ms, and neither is significantly different (Smirnov test, 5% level) from the histogram in *A* where the membrane was stepped directly to −30 mV.

Channel Open Times

Fig. 9 *A* shows histograms of open times for the channel shown in Fig. 7. Open times were measured for steps to +30 mV (Fig. 7 *A*, left) and for steps to −30 mV (Fig. 7 *A*, right). Open times are longer at +30 mV compared with steps to −30 mV; the mean open time at +30 mV is 42.3 ms, whereas at −30 mV it is only 18.6 ms. Superimposed on the histograms are single exponential curves with time constants of 42 ms (+30 mV) and 19 ms (−30 mV). Both histograms are reasonably well fit by first-order kinetics and are not significantly different (Lilliefors test, 5% level) from the superimposed exponentials, suggesting that the channel has only one open state and that the rate constants for leaving the open state are voltage dependent. This confirms our earlier observations on these channels (Cooper and Shrier, 1985).

In addition, we also tested whether the rate constants for leaving the open state varied with time, as this could give evidence that other mechanisms were involved in controlling open times. For example, if some additional inactivation process(es) started at the beginning of the voltage step, one might expect that open times of events that opened later in the step would be shorter than those events that opened at the beginning of the step (see Aldrich and Yellen, 1983). To test this, we measured open times of all events that opened at times greater than 30 ms after the beginning of the voltage step to +30 mV (most of these events were reopenings of the channel, see below). The histogram of open times for these later events are shown in Fig. 9 *B*. The mean open time was 37.7 ms and the histogram was not statistically different (Smirnov test, 5% level) from the histogram of the total population shown in Fig. 9 *A*. These results suggest that the rate constants for leaving the open state at +30 mV do not change with time.

Furthermore, we tested if open times were affected by the previous history of the membrane potential. For this experiment, open times were measured at −30 mV after the membrane had been depolarized from −90 to +30 mV for 50 ms (see Fig. 9 *C*); these open times were compared with values that were derived when the membrane was depolarized directly from −90 to −30 mV (see Fig. 9 *A*). The two histograms are not significantly different from each other which suggests that open times are governed by membrane potential, per se, and not by the method in which the membrane potential is attained. In addition, 53 events were still open upon stepping down from +30 to −30 mV (tails) (see Fig. 9 *C*) and the open times of these events were also not significantly different (Smirnov test, 5% level) from the other open times at −30 mV, suggesting that the rate constants for leaving the open state change almost instantaneously.

Channel Reopening

The tendency for the channel to reopen was measured by counting the number of openings on each step to +30 and −30 mV. The results are expressed as histograms in Fig. 10 *A* and indicate the frequency of steps with different numbers of openings (steps in which the channel did not open were not included in the histogram). It is clear that the frequency of reopening shows little voltage dependence and is not significantly greater at −30 mV compared with those at +30 mV. In some patches, there was very little reopening (see for example Fig. 12, and Cooper

and Shrier, 1985), and in other patches, the number of reopenings was much greater (Figs. 16 and 17, below). This suggests that possibly other factors govern channel reopening.

Closed Times

The closed times between successive openings are shown as histograms in Fig. 10 *B*. From this figure, it is clear that there are two components to the closed times; these

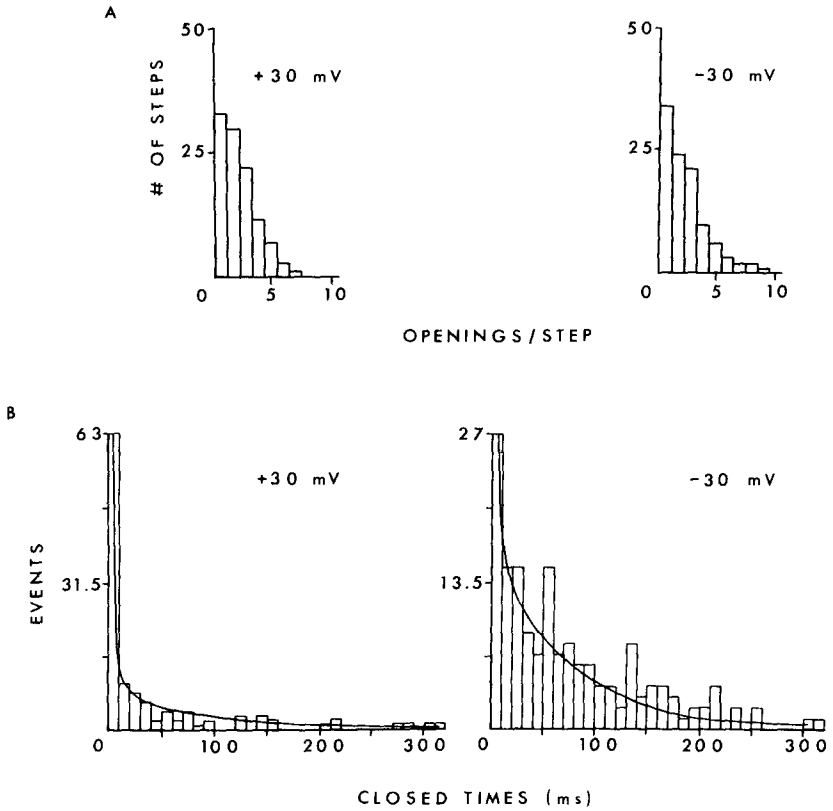

FIGURE 10. Reopenings and closed-time intervals. *A* shows histograms of the number of openings per step at +30 mV (*left*) and −30 mV (*right*) for the channel shown in Fig. 7. As this patch contained only one channel, all bins except the first represent reopenings of the channel. *B* shows histograms of closed-time intervals at +30 mV (*left*) and at −30 mV (*right*) for reopenings shown in Fig. 7. The solid lines represent curves drawn as the sum of two exponentials whose time constants are 3.5 and 75 ms. There were 117 intervals measured at +30 mV and 174 intervals measured at −30 mV.

histograms were fit by the sum of two exponentials, one whose time constant was 3.5 ms and the other whose time constant was 75 ms. This suggests that the channel closes to one of two states from which it could reopen before closing to an inactivated state from which no reopening would occur. While the time constants do not appear to show much voltage dependence, the probability of closing to one of these

two states does depend on voltage. At +30 mV, the proportion of events closing to the state with the fast time constant was 44%, whereas at −30 mV the proportion was 6.5%.

From the experiments shown in Figs. 7–10, we conclude that activation of the channel is fast and voltage-dependent, that the channel has only one open state whose closing rates are voltage dependent, that the channel has at least two closed states apart from an inactivated state, and that the channel reopening is not strongly voltage dependent. In addition, the channel can pass directly from the resting state to the inactivated state without going through the open state, and the probability for channels inactivating in this way is greater at lower depolarizations.

Activation Near Threshold

From Fig. 8 it is clear that activation is fast and steeply voltage dependent. Therefore, we measured activation at low depolarizations, near the threshold for activation of the A current; our macroscopic experiments and most reports on A currents in the literature indicate this to be at ~−50 mV. Fig. 11 shows the results from a patch containing five to six channels in which voltage steps were made to different voltages. Channels were rarely observed for steps to −60 mV (not shown) as this potential is presumably below the threshold for channel activation. However, further depolarization by 8 mV to −52 mV increased the number of openings. At this potential, the channels appeared brief in duration and opened with relatively long latencies. As the patch was depolarized a further 8 mV to −44 mV, the probability for opening increased; in addition, the channels stayed open longer (see Fig. 11) and opened with a shorter latency. As the patch was depolarized to −36 mV (see Fig. 11), the main effect was a further increase in the probability of opening, a decrease in channel latency, and an increase in channel open time.

Steady-State Inactivation

A test that we routinely performed to identify A channels was one for steady-state inactivation because, as mentioned above, a distinguishing feature of A channels is that they are almost completely inactivated by steady holding near the resting potential and require hyperpolarization to remove the inactivation. An example of this is shown in Fig. 12, where a membrane patch containing three A channels was held at three different potentials. At −90 mV holding potential, where inactivation is mostly removed, one to two channels opened on almost every step, whereas for the same patch held at −65 mV only a few steps opened channels. The ensemble averages for the three different holding potentials are shown in Fig. 12 *A*, and the relationship between the peak of the ensemble average and the holding potential are consistent with that found for macroscopic A currents shown in Fig. 2. The main effect of removal of inactivation at the single-channel level in these experiments was to increase the probability that A channels open upon membrane depolarization; the extent of inactivation had no apparent effect on the latency for the channel to open, or on the channel open time. Fig. 12 *B* shows measurements of channel open time evoked from the three different holding potentials and demonstrates that the mean open times are not different from each other and are similar to the decay of the ensemble average in this patch.

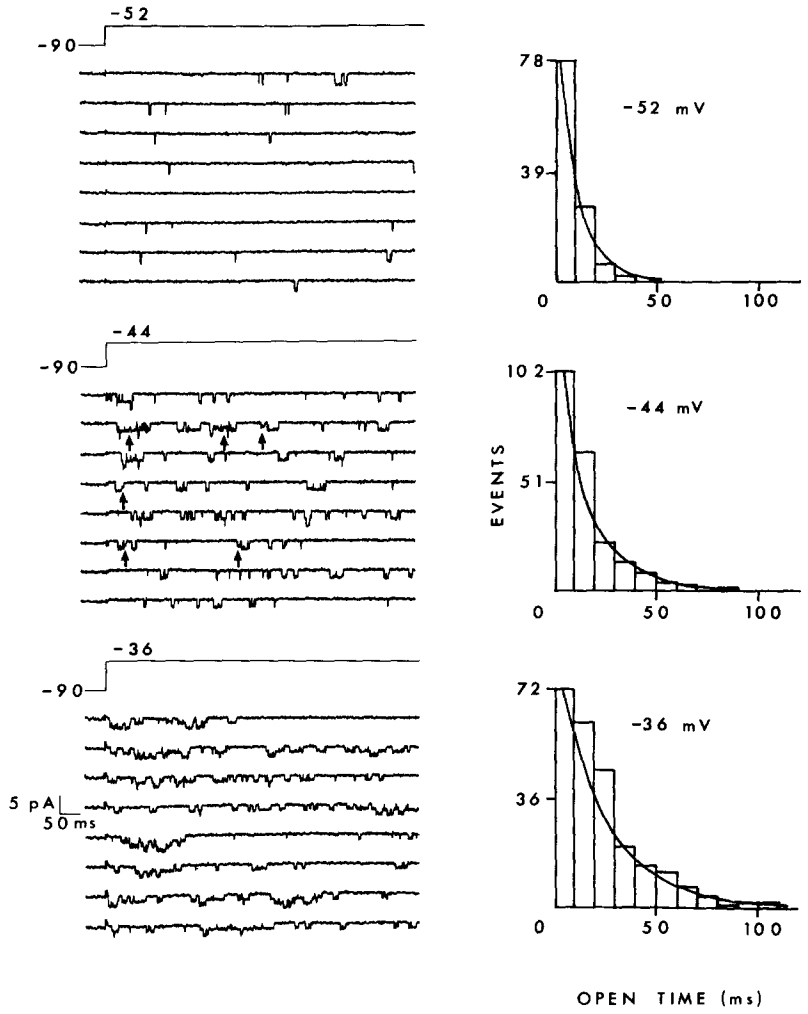

FIGURE 11. Threshold for activation and open times. This figure shows three sets of eight consecutive current traces in response to voltage steps from −90 to −52 mV (*top*), −44 mV (*middle*), and −36 mV (*bottom*). On the right of each set are histograms of the open times at the three potentials (n = 114 at −52 mV, n = 216 at −44 mV, and n = 238 at −36 mV). The solid lines represent single exponential curves with time constants equal to 11 ms for −52 mV, 17 ms for −44 mV, and 25 ms for −36 mV. Twelve percent of steps to −52 mV had no openings. The recording electrode contained 140 mM K and the channels open downwards (inward) as E_K = 0 mV. The currents were filtered at 1.25 kHz and sampled at 2.5 kHz. The arrows indicate substates.

Closed State to Inactivated State without Opening

The cumulative histogram of first latencies at −30 mV, shown in Fig. 8, reaches an asymptote at ~75%, suggesting that in 25% of the steps to this potential the channel goes from the closed to the inactivated state without opening (Aldrich et al., 1983). We tested this possibility directly in other patches by using a two-step protocol. An

example is shown in Fig. 13. In this experiment, 51 out of 125 of the first steps to −30 mV failed to activate channels; for these 51 steps, only four of the second steps activated channels (Fig. 13 *B*); if step 1 did not trigger an inactivation process then 36 of the second steps to +30 mV (or 70%) should have activated channels. These results indicate that the channels went directly from the resting state into an inactivated state at −30 mV without previously opening.

Deactivation

At the macroscopic level, we showed that steps to −40 mV for 130 ms inactivate the rapidly decaying component of the A current but does not affect the slower components which open when the membrane is further depolarized to +10 mV and

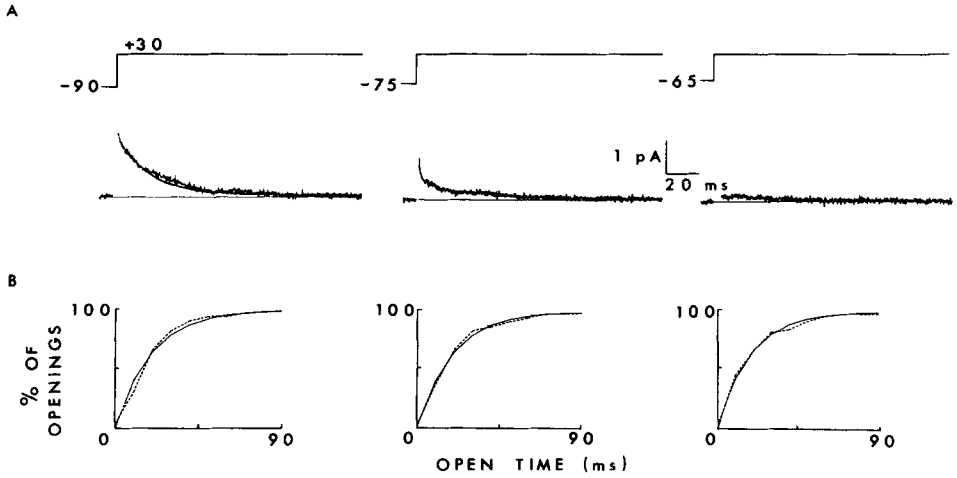

FIGURE 12. Removal of inactivation. This figure shows the effect of holding potential on the removal of inactivation of the channel. The membrane patch was held at three potentials −90 mV, −75 mV, and −65 mV and stepped to +30 mV. *A* shows the ensemble averages of the current for 90–100 steps at each holding potential. The solid line through the data for the step from −90 mV represents a curve drawn as a single exponential with a time constant of 21.3 ms. (*B*) The dotted curve shows the cumulative histograms for open times for each holding potential. The continuous line is an exponential fit [1 − exp (−t/19)]. The records in *A* and *B* were filtered at 1.5 kHz and sampled at 5 kHz.

requires seconds for inactivation (see Fig. 4). Once activated the slower component deactivates at −40 mV. Fig. 14 demonstrates deactivation at the single-channel level. When this patch was depolarized to +30 mV for 30 ms and then repolarized to −40 mV for 200 ms the channels closed; the few openings present at the beginning of the step to −40 mV in Fig. 14 *C* represent tail currents. Subsequent depolarization to +30 mV resulted in channels reopening, indicating that during the 200 ms at −40 mV some channels were deactivated and not inactivated. Results similar to these were obtained on six other patches.

In 10 other experiments, the rate of deactivation was examined at −90 mV and found to be very fast. An example is shown in Fig. 15. In this experiment, the channels shut off instantaneously when repolarized to −90 mV. The lack of openings at

−90 mV is presumably because this potential is well below the activation range for the channel (see Fig. 11).

Reversibility of Inactivation Modes

In some patches, we observed channels that would activate once and then inactivate, and in other patches we observed channels that required several seconds to close to

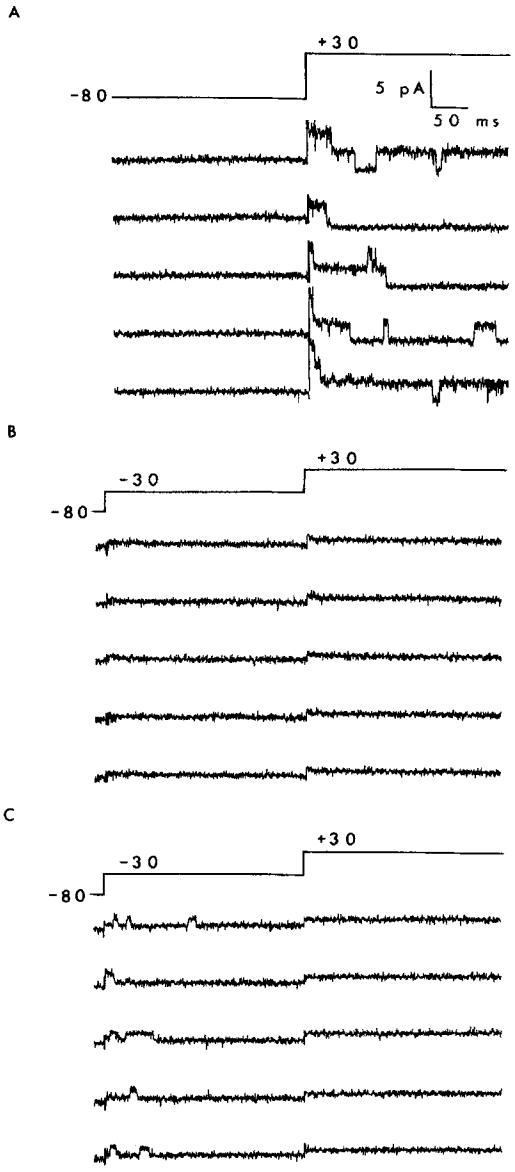

FIGURE 13. Closed to inactivate. *A* shows five consecutive current traces in response to voltage steps from −80 to +30 mV. *B* is the same patch as in *A* and shows five current traces in response to voltage steps from −80 to −30 mV for 500 ms and then to +30 mV. These records show that the channel can inactivate without opening first (see text). *C* is the same patch as in *A* and *B*, and shows five current traces in response to the same protocol as in *B*. These records show that when the channel opens at −30 mV it can be clearly detected. The recording electrode contained 5.4 mM K and the voltage steps were delivered every 2.5 s. The currents were filtered at 1 kHz and sampled at 2 kHz.

the inactivated state. In a few patches ($n = 4$), however, we observed that the channel apparently went from one inactivation mode to another reversibly. An example from one such patch is shown in Fig. 16. This patch contains two channels; we made repeated steps to +30 mV and we estimated that the probability that a channel opened was ~0.6. For most steps the channel would activate with a short latency and close to an inactivated state with few reopenings; however, interspersed between these steps was a series in which a channel would open and close repeatedly (see Fig.

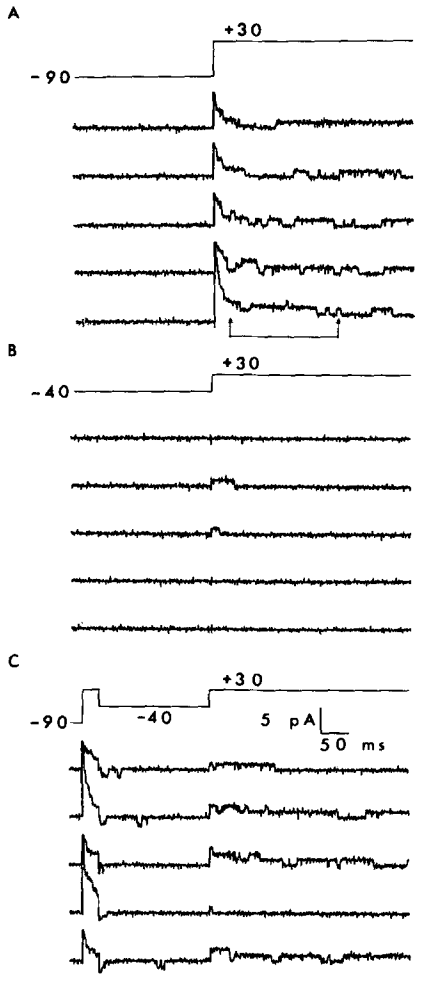

FIGURE 14. Deactivated state. *A* shows five consecutive current traces in response to voltage steps from −90 to +30 mV. *B* shows five consecutive current traces from the same patch in response to voltage steps from −40 to +30 mV. *C* shows five consecutive current traces in response to voltage steps from −90 to +30 mV for 30 ms, then back to −40 mV for 200 ms and back up to +30 mV for 400 ms. The currents at +30 mV are upward (outward) while those at −40 mV are downward (inward); ($E_K = 0$ mV for this patch and the recording electrode contained 140 mM K). The portion between the arrows in *A* represent the period corresponding to the step back to −40 mV in *C*. The records were filtered at 1.5 kHz and sampled at 3 kHz.

16). This burst of activity would continue for 3–10 steps and then the activity would subside, and for the subsequent several steps the channel opened and closed to an inactivated state without reopening as in the steps before the burst of activity. At some time later, there was another burst of activity that lasted for another 3–10 steps and then subsided.

These data suggest that the channel could go reversibly into a slow inactivation

mode. However, with repeated steps, it was difficult to determine how long it took before the channel inactivated because after each step the potential was returned to −90 mV, which would remove any inactivation that might have occurred. Therefore, to determine the time for inactivation when the channel was in this mode we left the step depolarized at +30 mV until the channel fully inactivated. Fig. 16 (right) shows a continuous record of the current when the voltage step was left on for 11 s. As can be seen in this example, the channel shuttled back and forth between open and closed states for 8.3 s before inactivating.

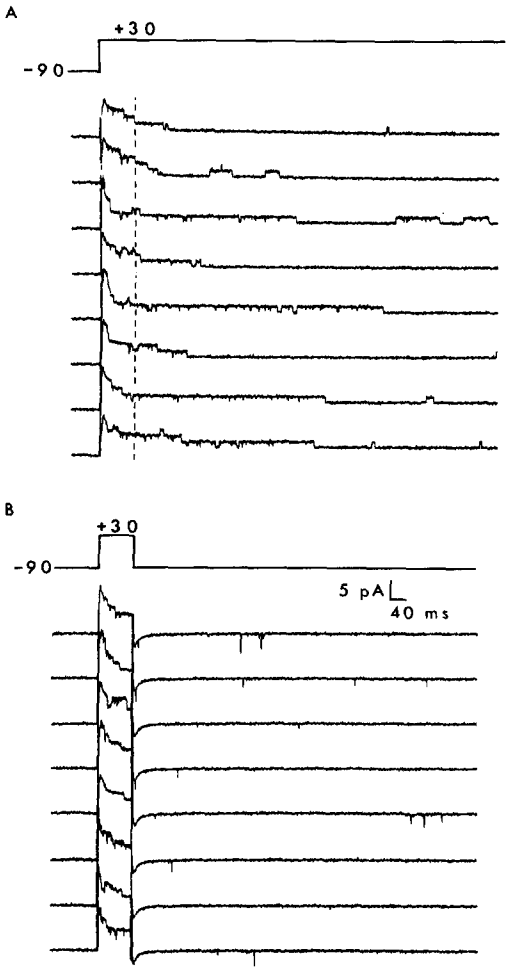

FIGURE 15. Closed at hyperpolarized voltages. This figure shows two sets of eight consecutive current traces from the same patch in response to voltage steps from −90 to +30 mV. In *A* the voltage step was on for 800 ms and in *B* the step was on for 80 ms. The dotted line in *A* occurs at 80 ms for comparison with *B* and shows that most records have channels open after that time. In *B* the rapid events may represent attempts at channel opening and deflect downwards because E_K = 0 mV for this patch. The records have not been corrected for capacity transients or leakage and were filtered at 1 kHz and sampled at 2 kHz.

Slow Inactivation

As shown above, the inactivation time course of the macroscopic A current is complex and can contain a very slow component that requires seconds for inactivation. To test whether this slow component could result from the same single channels that we described above, we applied long 10–12-s depolarizing pulses to membrane

patches that had A channels. An example is shown in Fig. 17. Fig. 17 *A* demonstrates that while A channels can inactivate rapidly in tens of milliseconds, some A channels undergo very long inactivation. A similar slow inactivation has also been recently shown for Na channels on muscle (Kunze et al., 1985; Patlak and Ortiz, 1985), however, the frequency of Na channels undergoing slow inactivation is more than two orders of magnitude less than what we observed for A channels.

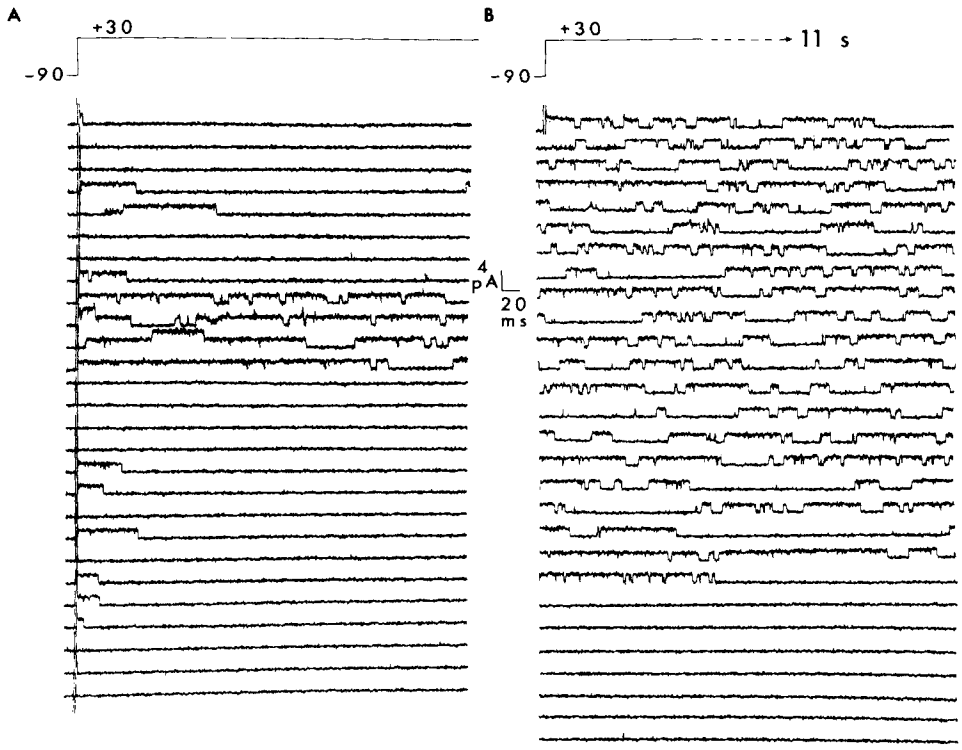

FIGURE 16. Slow inactivation. *A* shows 27 consecutive current traces from a patch that contains two channels in response to repetitive voltage pulses from −90 to +30 mV for 400 ms delivered every 2 s. In this sequence, most traces show that the channels inactivate rapidly; however, in four consecutive traces the channels do not appear to inactivate. *B* shows a continuous 11-s record from the same patch. The traces have been rastered so that the end of one line is continuous with the beginning of the line below it. The recording electrode contained regular 5.4 mM K and the records were filtered at 1.5 kHz and sampled at 5 kHz.

Fig. 17 shows the ensemble average of 43 records in response to depolarizing steps to +30 mV, like those shown in Fig. 17 *A*. This average bears close resemblance to the macroscopic A current in response to long pulses, such as that shown in Fig. 4. Most likely, the time course of decay of the macroscopic A current depends on the proportion of A channels in the membrane that inactivate in the different modes.

DISCUSSION

In this paper, we provide evidence that the A currents in nodose neurons are made up of a single class of channels that have complex kinetics. At the macroscopic level, we show that the decline of the A currents can be fit by the sum of three exponentials that are the result of A channels inactivating in three different modes. The

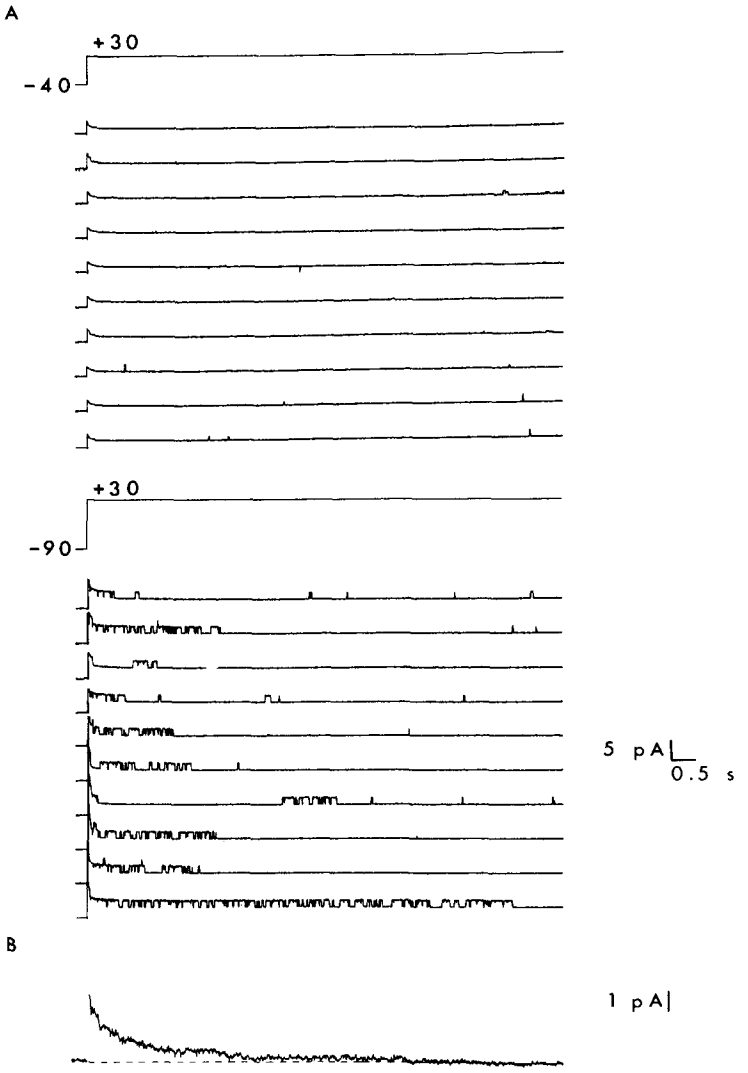

FIGURE 17. A channels in response to long steps. *A* shows two sets of 10 consecutive current traces in response to 10-s voltage steps to +30 mV from holding potentials of −40 mV (*upper set*) and −90 mV (*lower set*) recorded in 5.4 mM K. *B* shows the ensemble average of 43 voltage steps from −90 to +30 mV. The records were filtered at 0.1 kHz and sampled at 0.2 kHz.

more rapidly inactivating components of the A current are similar to A currents first described in molluscan neurons (Connor and Stevens, 1971; Neher, 1971; and reviewed by Adams et al., 1980) and recently shown to be present in several mammalian neurons (for example, Kostyuk et al., 1981; Gustafsson et al., 1982; Segal and Barker, 1984; Belluzi et al., 1985; Bossu et al., 1985; Zbicz and Weight, 1985), and in several nonneuronal cells including rat lactotrophs of the anterior pituitary (Lingle et al., 1986), crista terminalis of rabbit heart (Giles and van Ginnekan, 1985) and newt thrombocytes (Kawa, 1987).

In addition, we have identified a slow component of the A current from ensemble averages of patches containing A channels and from macroscopic whole-cell currents. Records from several other studies show evidence of a slow component suggesting that it may be a general feature of A currents (Segal and Barker, 1984; Lingle et al., 1986; Numann et al., 1987; Mayer and Sugiyama, 1988). At the macroscopic level this slowly inactivating part of the A current conceivably could be interpreted as a component of other K currents. For example, the delayed rectifier current on frog skeletal muscle (Adrian et al., 1970) and on hippocampal neurons (Segal and Barker, 1984) have been shown to undergo inactivation over seconds. However, in our experiments, we found that IK does not inactivate. In neurons that did not express A currents, we could show that holding at hyperpolarized voltages did not remove any inactivation of the delayed rectifier and that currents evoked by depolarizing steps from -40 mV were not different from currents evoked when holding at -90 mV. From our single-channel measurements, we show that A channels activate rapidly upon depolarization to $+20$ or $+30$ mV. The peak probability that the channel opens is ~0.6—0.7 at $+30$ mV and is reached within 5 ms at 22°C, and the latencies for first opening are steeply voltage dependent. A channels have only one open state and the rate constants for leaving the open state are voltage dependent.

In this paper we showed that inactivation of A channels occur in three main ways. Some A channels close directly to the inactivated state with little reopening; these channels underlie the rapid decay of the macroscopic current (Cooper and Shrier, 1985). Other A channels open and close to one of two closed, or deactivated, states a few times before they inactivate. One closed state has a rapid (3.5 ms) time constant, the other closed state has a time constant (75 ms) more than an order of magnitude greater, and the probability of closing to one of these two states was voltage dependent: the channel entered the rapid closed state more frequently at $+30$ mV compared with -30 mV. Ensemble averages of A channels that inactivate in this way had time constants of 100–350 ms. In addition, we observed A channels that inactivated in a slow mode in which the channel opened and closed several hundred times and required seconds for inactivation.

The A channels on nodose neurons have an open-channel conductance of 22 pS when recorded in cell-attached configurations and exposed to 5.4 external mM K, and measured 40 pS when exposed to 140 mM external K; and, as shown for inward-rectifying K channels (Hagiwara and Takahashi, 1974; Ohmori, 1978; Fukushima, 1982; Sakmann and Trube, 1984), the conductance of A channels varies with the square root of the external K concentration. In addition, we observed that the

channel could exist in a lower conducting state, although the frequency of observing this substate was low and the time spent in the substate was brief.

A channels on rat nodose neurons are similar to those on rat DRG neurons (Kasai et al., 1986), both in their conductance and the time required for inactivation; some A channels on rat DRG neurons require seconds for inactivation and may underlie the very slow component of the macroscopic A current observed on these neurons (Mayer and Sugiyama, 1988). The A channels on nodose neurons also appear similar to Kw channels recorded on rat pheochromocytoma cells (PC12) (Hoshi and Aldrich, 1988*b*). Kw channels have a conductance (14–18 pS) that is close to that of A channels (22 pS); these channels activate rapidly upon depolarization to positive potentials and their latencies are very voltage dependent. The values of first latencies for Kw channels are similar to A channels on nodose neurons at the corresponding potentials, the time constants for inactivation of Kw channels (40–80 ms) are also similar to what we observed for some A channels. In addition, Kw channels have only one open state and the rate constant for leaving the open state are voltage dependent; however, the closing rates for Kw channels appear faster than do those for A channels. A channels also compare with FK channels on bovine chromaffin cells (Marty and Neher, 1985) in that FK channels have a similar conductance (18 pS), activate rapidly upon depolarization, and have opening probabilities of 0.6 at +30 mV.

FK and Kw channels differ in the time required for inactivation. Kw channels inactivate in ~60 ms, as do some FK channels, however, other FK channels require much longer times. This difference in the time for inactivation between FK and Kw channels may be similar to the difference in the time for inactivation of A channels on nodose neurons.

Analogies have been made between the A current and the fast inward Na current at the macroscopic level. And, in fact, recently a cDNA from Shaker mutants of *Drosophila,* thought to represent part of the gene for the A channels, has been sequenced, and the region believed to be the voltage sensor shows homologies with genes for Na channels (Baumann et al., 1987; Papazian et al., 1987; Catteral, 1988). Further similarities between A channels and Na channels come from studies that show that agents such as *N*-bromoacetamide (NBA) and papain, which slow the inactivation of Na channels (reviewed by French and Horn, 1983), also slow the inactivation of A currents (Kawa, 1987; Matheson and Carmeliet, 1988). At the single-channel level, similarities also exist between the A channels reported here and single Na channels. For example, at large depolarizations, Na channels activate rapidly and then inactivate irreversibly, each channel opening only once before becoming almost completely inactivated (French and Horn, 1983). At lower depolarizations, A channels resemble Na channels expressed by GH3 cells and skeletal muscle (Horn and Vandenberg, 1984; Vandenberg and Horn, 1984; Patlak and Ortiz, 1985) in that the channels open a few times before inactivating. In addition, both A channels and Na channels can enter kinetic modes where inactivation is slowed for many hundreds of milliseconds (Kunze et al., 1985; Patlak and Ortiz, 1985). However, the frequency of this occurring is orders of magnitude lower for Na channels (Patlak and Ortiz, 1985). A channels on nodose neurons seem to differ from Na channels expressed on neuroblastoma, where at low depolarizations Na channels activate with

relatively long latencies and close to an inactivated state and the mean open times are relatively insensitive to membrane potential (Aldrich et al., 1983; Aldrich and Stevens, 1987). However, we showed that like Na channels on neuroblastomas (Aldrich and Stevens, 1983), A channels can go directly from the resting, or closed, state to the inactivated state without opening, and that the probability that A channels inactivate in this way is greater at less depolarized membrane potentials.

The reason for the variability in the inactivation between different A channels is unclear. In some patches, we observed that A channels could go reversibly from a mode where inactivation occurred rapidly to a mode where inactivation required seconds, suggesting that perhaps A channel inactivation is subject to modulation by intracellular factor(s). For example, there is evidence that suggests that A currents can be modulated by cAMP (Strong, 1984; Strong and Kaczmarek, 1986; but see also Coombs and Thompson, 1987; Hoshi et al., 1988). In this context, it has been shown that resting newt thrombocytes have A currents that inactivate rapidly, but upon activation by plasminogen activator the A current inactivates orders of magnitude slower (Kawa, 1987). An alternative possibility for why the same basic channel may gate in a fast or a slow mode is that these channels represent different subclasses of A channels that are structurally similar in many respects but differ in the part of the molecule that controls channel inactivation. In this context, recent work on genes from Shaker mutants of *Drosophila* suggest that different gene products, and by implication A channels, can be produced from A channel genes by alternative splicing (Kamb et al., 1987; Pongs et al., 1988; Schwartz et al., 1988; Timpe et al., 1988; Butler et al., 1989). This could conceivably lead to A channels that differ in their inactivation properties.

We thank Ms. Brigitte Pie for technical assistance with the cultures, and Drs. C. R. Bader, D. Bertrand, L. Bernheim, R. Schlichter, Ms. Sarah McFarlane, and Linda Cooper for providing helpful comments on earlier versions of the manuscript.

This work was supported by individual grants from the Medical Research Council of Canada to E. Cooper and A. Shrier; E. Cooper is a senior chercheur of the Fonds de la Recherche en Santé du Quebec.

Original version received 19 August 1988 and accepted version received 7 April 1989.

REFERENCES

Adams, D. J., S. J. Smith, and S. H. Thompson. 1980. Ionic currents in molluscan neurons. *Annual Review of Neuroscience.* 3:141–167.

Adrian, R. H., W. K. Chandler, and A. L. Hodgkin. 1970. Voltage clamp experiments in striated muscle fibres. *Journal of Physiology.* 208:607–644.

Aldrich, R. W., D. P. Corey, and C. F. Stevens. 1983. A reinterpretation of mammalian sodium channel gating based on single channel recording. *Nature.* 306:436–441.

Aldrich, R. W., and C. F. Stevens. 1983. Inactivation of open and closed sodium channels determined separately. *Cold Spring Harbor Symposium on Quantitative Biology.* 48:147–153.

Aldrich, R. W., and C. F. Stevens. 1987. Voltage-dependent gating of single sodium channels from mammalian neuroblastoma cells. *Journal of Neuroscience.* 7:418–431.

Aldrich, R. W., and G. Yellen. 1983. Analysis of nonstationary channel kinetics. *In* Single Channel Recording. B. Sakmann and E. Neher, editors. Plenum Publishing Corp., New York. 287–299.

Akaike, H. 1974. A new look at the statistical model identification. *IEEE Transaction in Automatic Control.* AC-19:716–723.

Baccaglini, P. I., and E. Cooper. 1982. Electrophysiological studies of new-born rat nodose neurones in culture. *Journal of Physiology.* 324:429–439.

Baumann, A., I. Krah-Jentgens, R. Muller-Holtkamp, R. Seidel, N. Kecskemethy, J. Casal, A. Ferrus, and P. Pongs. 1987. Molecular organization of the maternal effect region of the shaker complex of *Drosophila:* characterization of an IA channel transcript with homology to vertebrate Na channel. *EMBO Journal.* 6:3419–3429.

Belluzzi, O., O. Sacchi, and E. Wanke. 1985. A fast transient outward current in the rat sympathetic neurone studied under voltage clamp conditions. *Journal of Physiology.* 358:91–108.

Bocchini, V., and P. V. Angeletti. 1969. The nerve growth factor: purification as an 80,000–molecular-weight protein. *Proceedings of the National Academy of Sciences.* 64:787–794.

Bossu, J. L., J. L. Dupont, and A. Feltz. 1985. IA current compared to low threshold calcium current in cranial sensory neurons. *Neuroscience Letters.* 62:249–254.

Bossu, J. L., and A. Feltz. 1984. Patch clamp studies of the tetrodotoxin-resistant sodium current in group c sensory neurons. *Neuroscience Letters.* 51:241–246.

Butler, A., A. Wei, K. Baker, L. Salkoff. 1989. A family of putative potassium channel genes in *Drosophila. Science.* 243:943–947.

Catterall, W. A. 1988. Structure and function of voltage-sensitive ion channels. *Science.* 242:50–61.

Connor, J. A., and C. F. Stevens. 1971. Voltage clamp of a transient outward current in gastropod neuronal somata. *Journal of Physiology.* 213:21–30.

Conover, W. J. 1980. Practical Nonparametric Statistics. 2nd Ed. John Wiley & Sons, New York.

Coombs, J., and S. Thompson. 1987. Forskolin's effect on transient K current in nudibranch neurons is not reproduced by cAMP. *Journal of Neuroscience.* 7:443–452.

Cooper, E. 1984. Synapse formation among developing sensory neurons from rat nodose ganglia grown in tissue culture. *Journal of Physiology.* 351:263–274.

Cooper, E., and A. Shrier. 1985. Single-channel analysis of fast transient potassium currents from nodose neurons. *Journal of Physiology.* 369:199–208.

French, R. J., and R. Horn. 1983. Sodium channel gating: models, mimics, and modifiers. *Annual Review of Biophysics and Bioengineering.* 12:319–356.

Fukushima, Y. 1982. Blocking kinetics of the anamolous potassium rectifier of tunicate eggs studied by single channel recording. *Journal of Physiology.* 331:311–331.

Giles, W. R., and A. C. G. van Ginneken. 1985. A transient outward current in isolated cells from the crista terminalis of rabbit heart. *Journal of Physiology.* 368:243–264.

Gustafsson, B., M. Galvan, P. Grafe, and H. A. Wigstrom. 1982. A transient outward current in a mammalian central neuron blocked by 4-aminopyridine. *Nature.* 299:252–254.

Hagiwara, S., K. Kusano, and N. Saito. 1961. Membrane changes of onchidium nerve cell in potassium-rich media. *Journal of Physiology.* 155:470–489.

Hagiwara, S., and K. Takahashi. 1974. The anomalous rectification and cation selectivity of the membrane of the starfish egg cell. *Journal of Membrane Biology.* 18:61–80.

Hamill, O. P., A. Marty, E. Neher, B. Sakmann, and F. J. Sigworth. 1981. Improved patch clamp techniques for high resolution current recording from cells and cell free membrane patches. *Pflügers Archiv.* 391:85–100.

Horn, R., and C. A. Vandenberg. 1984. Statistical properties of single sodium channels. *Journal of General Physiology.* 84:505–534.

Hoshi, T., and R. W. Aldrich. 1988*a*. Voltage-dependent K currents and underlying single K channels in pheochromocytoma cells. *Journal of General Physiology.* 91:73–106.

Hoshi, T., and R. W. Aldrich. 1988*b*. Gating kinetics of four classes of voltage-dependent K channels in pheochromocytoma cells. *Journal of General Physiology.* 91:107–131.

Hoshi, T., S. S. Garber, and R. W. Aldrich. 1988. Effect of forskolin on voltage-gated K channels is independent of adenylate cyclase activation. *Science.* 240:1652–1655.

Hunter, I. W., and R. W. Kearney. 1984. NEXUS: a computer language for physiological system and signal analysis. *Computers in Biology and Medicine.* 14:385–401.

Ikeda, S. R., and G. G. Schofield. 1987. Tetrodotoxin-resistant sodium current of rat nodose neurones: monovalent cation selectivity and divalent cation block. *Journal of Physiology.* 389:255–270.

Kamb, A., L. E. Iverson, and M. A. Tanouye. 1987. Molecular characterization of Shaker, a *Drosophila* gene that encodes a potassium channel. *Cell.* 50:405–413.

Kasai, H., M. Kameyama, K. Yamaguchi, and J. Fukuda. 1986. Single transient K channels on mammalian sensory neurons. *Biophysical Journal.* 49:1243–1247.

Kawa, K. 1987. Transient outward current and changes of their gating properties after cell activation in thrombocytes of the newt. *Journal of Physiology.* 385:189–205.

Kostyuk, P. G., N. S. Veselovsky, S. A. Fedulova, and A. Y. Tsyndrenko. 1981. Ionic currents in the somatic membrane of rat dorsal root ganglion neurons. III. Potassium current. *Neuroscience.* 6:2439–2444.

Kunze, D. L., A. E. Lacerda, D. L. Wilson, and A. M. Brown. 1985. Cardiac Na currents and the inactivation, reopening, and waiting properties of single cardiac Na channels. *Journal of General Physiology.* 86:691–719.

Lingle, C. J., S. Sombati, and M. E. Freeman. 1986. Membrane currents in identified lactotrophs of rat anterior pituitary. *Journal of Neuroscience.* 6:2995–3005.

Marty, A., and E. Neher. 1985. Potassium channels in cultured bovine adrenal chromaffin cells. *Journal of Physiology.* 367:117–141.

Matheson, D. R., and P. Carmeliet. 1988. Modification of K channel inactivation by papain and *N*-bromoacetamide. *Biophysical Journal.* 53:641–645.

Mayer, M., and K. Sugiyama. 1988. A modulatory action of divalent cations on transient outward current in cultured rat sensory neurons. *Journal of Physiology.* 396:417–433.

Neher, E. 1971. Two fast transient current components during voltage clamp of snail neurons. *Journal of General Physiology.* 58:36–53.

Numann, R. E., W. J. Wadman, and R. K. S. Wong. 1987. Outward currents of single hippocampal cells from adult guinea-pig. *Journal of Physiology.* 393:331–353.

Ohmori, H. 1978. Inactivation kinetics and steady-state current noise in the anamolous rectifier of the tunicate egg cell membrane. *Journal of Physiology.* 281:77–99.

Papazian, D. M., T. L. Schwartz, B. L. Tempel, Y. N. Jan, and L. Y. Jan. 1987. Cloning of genomic and complementary DNA from Shaker, a putative potassium channel gene from *Drosophila*. *Science.* 237:749–753.

Patlak, J., and R. Horn. 1982. Effects of *N*-bromoacetamide on single sodium channel currents in excised membrane patches. *Journal of General Physiology.* 79:333–351.

Patlak, J. B., and M. Ortiz. 1985. Two modes of late Na channel currents in frog sartorius muscle. *Journal of General Physiology.* 87:305–326.

Pongs, O., N. Kecskemethy, R. Muller, I. Krah-Jentgens, A. Baumann, H. H. Kiltz, I. Canal, S. Llamazares, and A. Ferrus. 1988. Shaker encodes a family of putative potassium channel proteins in the nervous system of *Drosophila*. *EMBO Journal.* 7:1087–1096.

Sakmann, B., and G. Trube. 1984. Conductance properties of single inwardly rectifying potassium channels in ventricular cells from guinea-pig heart. *Journal of Physiology.* 347:641–657.

Schwartz, T. L., B. L. Tempel, D. M. Papazian, Y. N. Jan, and L. Y. Jan. 1988. Multiple potassium-channel components are produced by alternative splicing at the Shaker locus in *Drosphila*. *Nature*. 331:137–142.

Segal, M., and J. L. Barker. 1984. Rat hippocampal neurons in culture: potassium conductances. *Journal of Neurophysiology*. 51:1409–1433.

Sigworth, F. J. 1983. Electronic design of the patch clamp. *In* Single Channel Recording. B. Sakmann, and E. Neher, editors. Plenum Publishing Corp., New York. 3–35.

Solc, C. K., W. N. Zagotta, and R. W. Aldrich. 1987. Single channel and genetic analyses reveal two distinct A type potassium channels in *Drosophila*. *Science*. 236:1094–1098.

Standen, N. B., P. R. Stanfield, and T. A. Ward. 1985. Properties of single potassium channels in vesicles formed from sarcolemma of frog skeletal muscle. *Journal of Physiology*. 365:339–358.

Strong, J. A. 1984. Modulation of potassium current kinetics in bag neurons of *Aplysia* by an activator of adenylate cyclase. *Journal of Neuroscience*. 4:2772–2783.

Strong, J. A., and L. M. Kaczmarek. 1986. Multiple components of delayed potassium current in peptidergic neurons of *Aplysia:* modulation by an activator of adenylate cyclase. *Journal of Neuroscience*. 6:814–822.

Taylor, P. S. 1987. Selectivity and patch measurements of A-current channels in *Helix aspersa* neurons. *Journal of Physiology*. 388:437–447.

Timpe, L. C., T. L. Schwartz, B. L. Tempel, D. M. Papazian, Y. N. Jan, and L. Y. Jan. 1988. Expression of functional potassium channels from Shaker cDNA in *Xenopus* oocytes. *Nature*. 331:143–145.

Vandenberg, C. A., and R. Horn. 1984. Inactivation viewed through single sodium channels. *Journal of General Physiology*. 84:535–564.

Zbicz, K. L., and F. Weight. 1985. Transient voltage and calcium dependent outward currents in hippocampal CA3 pyramidal neurons. *Journal of Neurophysiology*. 53:1038–1058.